Journal of Organometallic Chemistry 693 (2008) 2942–2948

Contents lists available at ScienceDirect

Journal of Organometallic Chemistry

journal homepage: www.elsevier.com/locate/jorganchem

CVD synthesis of nitrogen doped carbon nanotubes using ferrocene/aniline mixtures

Edward N. Nxumalo, Vincent O. Nyamori, Neil J. Coville *

DST/NRF Centre of Excellence in Strong Materials and the Molecular Sciences Institute, School of Chemistry, University of the Witwatersrand, Private Bag 3, Johannesburg, Wits 2050, South Africa

ARTICLE INFO

Article history:
Received 11 April 2008
Received in revised form 4 June 2008
Accepted 12 June 2008
Available online 18 June 2008

Keywords:
Carbon nanotubes
Shaped carbon nanomaterials
4-Ferrocenylaniline
Nitrogen doping
Ferrocene
Aniline

ABSTRACT

Nitrogen doped carbon nanotubes (N-CNTs) have been synthesized by the chemical vapour deposition (CVD) floating catalyst method using either 4-ferrocenylaniline or mixtures of varying concentrations of ferrocene/aniline together with toluene as added carbon source. The N-CNTs produced are less stable (thermal gravimetric analysis measurements), less graphitic and more disordered (transmission electron microscope measurements) than their undoped counterparts. The ratio of the Raman D- and G-band intensities increase with the nitrogen concentration used during the CNT growth. Furthermore, the transmission electron microscope (TEM) studies reveal that the CNTs are multi-walled (MW), and that the diameters of the N-MWCNTs can be controlled by systematically varying the concentrations of the nitrogen source. The TEM analysis also revealed that when ferrocenylaniline and ferrocene/aniline reactions are compared at similar Fe/N ratios, higher N doping levels are achieved (*ca.* 2–5×) when ferrocenylaniline is the catalyst.

1. Introduction

Carbon nanotubes (CNTs) and related structured carbon nanomaterials (spheres, fibers, horns, cages etc.) have been actively studied since the synthesis and identification of single-walled carbon nanotubes (SWCNTs) [1]. Much of the subsequent work in this area has been driven by the possible uses of the carbon materials in polymer blends, as light weight and conducting materials, as catalyst supports etc. [2]. Indeed recent reports reveal that demand for these carbon materials is increasing and that the industrial production of CNTs in the ton scale is now underway [3].

An analysis of the current literature reveals that the chemical vapour deposition (CVD) floating catalyst approach is the common method used to make CNTs on a large scale [4,5]. In this process a carbon source and a catalyst are passed through a hot quartz tube where the carbon source decomposes to form shaped carbon nanomaterials (SCNMs), in particular CNTs. This CVD methodology avoids the use of a catalyst support and the subsequent support removal procedures. The catalyst required to achieve this result is typically a volatile organometallic complex such as ferrocene (FcH) or $Fe(CO)_5$ [6]. Surprisingly, to date, little has been reported on the variation of the catalyst source on CNT synthesis procedures and a systematic approach using classical ligand effects has been little investigated [7]. In recent studies we and others have been using alternative organometallic complexes to ferrocene to synthesise CNTs by the floating catalyst method [8,9]. Interestingly most of these studies have focused on *ferrocene derivatives* as they provide a facile means of adding elements such as carbon and sulfur into the reactant stream. For example, a recent study reports a method of using a hetero atom (sulfur) to modify multi-walled carbon nanotube (MWCNT) synthesis using a modified sulfur containing ferrocene catalyst acting as both a catalyst and a carbon source [10].

When a hetero atom is *inserted into the backbone* of a CNT, the symmetry of the tube is modified and the structure and properties are altered [11]. Introduction of foreign atoms into the walls of CNTs was first performed by Stephen et al. [12], who doped CNTs with nitrogen (and boron) using arc discharge procedures. Incorporation of N into the CNT lattice can result in the enhancement of the electrical properties of the CNTs [13], which make them promising candidates for electronic devices [14]. Nitrogen doped carbon nanotubes (N-CNTs) are known to be exclusively conducting, showing n-type semiconducting characteristic [15]. Doping is also an important procedure to fine-tune the surface properties of CNTs. The doping of CNTs thus provides a unique entry into the chemistry of CNTs. In particular doping of CNTs with N permits the chemical reactivity of the CNT to be altered as would be expected by N insertion into any graphitic material, hence broadening the horizon of CNT chemistry.

N-Containing CNTs have been prepared by a template synthesis using a polyacrylonitrile precursor [16]. Recently, Point et al. [17], synthesized N-CNTs by electron cyclotron resonance CVD. Long strands of N-CNTs that agglomerated into bundles have been prepared *via* thermal decomposition of a ferrocene/ethanol/benzylamine solution [18]. Whilst doping is a crucial process to alter

* Corresponding author.
E-mail address: neil.coville@wits.ac.za (N.J. Coville).

0022-328X/$ - see front matter © 2008 Elsevier B.V. All rights reserved.
doi:10.1016/j.jorganchem.2008.06.015

the properties of CNTs, the challenge is to control the amount of N inserted into the tubes.

In this publication, we wish to report on the use of ferrocene (FcH)/aniline ($PhNH_2$) solutions to synthesize N-CNTs and other carbon species. We also report on the use of 4-ferrocenylaniline ($FcPhNH_2$) as both the N source and catalyst to grow N-CNTs. In particular, the effect of varying the N source concentration (0–25 wt.%) on the types and yield of CNTs and other SCNMs produced has been investigated. Characterization of the as-synthesized N-CNTs was achieved by conventional techniques. To the best of our knowledge, other than the use of metal porphyrin complexes [19], studies in which *organometallic precursors containing nitrogen* are used in the synthesis of N-CNTs have not been previously exploited.

2. Experimental

The precursor for 4-ferrocenylaniline i.e. 4-nitrophenyferrocene was prepared as described previously in 33% yield [20]. 4-Ferrocenylaniline was obtained by catalytic reduction of 4-nitrophenylferrocene in 66% yield and characterized by IR and NMR spectroscopy [21].

The crystal structure of 4-ferrocenylaniline was determined from single crystals grown from a mixture of dichloromethane and hexane. The 4-ferrocenylaniline crystals were obtained as orange needles with a melting point of 159 °C. Intensity data were collected on a Bruker APEX II CCD area detector diffractometer with graphite monochromated Mo Kα radiation (50 kV, 30 mA) using the APEX 2 [22] data collection software. The collection method involved ω-scans of width 0.5° and 512 × 512 bit data frames. Data reduction was carried out using the program SAINT+ and face indexed absorption corrections were made using XPREP [23]. The crystal structure was solved by direct methods using SHELXTL [24]. Non-hydrogen atoms were first refined isotropically followed by anisotropic refinement by full matrix least-squares calculations based on F^2 using SHELXTL. Hydrogen atoms were first located in the difference map then positioned geometrically and allowed to ride on their respective parent atoms. Diagrams and publication material were generated using SHELXTL, PLATON [25] and ORTEP-3 [26].

The CVD floating catalyst method was used for the synthesis of N-CNTs. Growth of the CNTs was carried out in a tubular furnace in a horizontal quartz tube (with dimensions of 800 mm and 28 mm) at atmospheric pressure (Fig. S1; Supplementary material). The temperature inside the reactor was kept at 900 °C and this was determined by means of a thermocouple positioned in the middle of the furnace. Typically, the quartz tube was heated to the desired temperature in 5% H_2 in argon (v/v) (AFROX) at a constant rate to remove the air from the system. The gases were flowed through the reactor at a controlled flow rate of 100 mL/min using an injection method. Solutions of toluene and 4-ferrocenylaniline (or ferrocene/aniline) were prepared and transferred to a 10 mL syringe driven by a SAGE pump. The ferrocenyl solutions were then injected into the high temperature zone of the furnace at an injection rate of 0.8 mL/min through a quartz water cooled system [27]. The reactor was then allowed to cool and the carbonaceous material was collected from the walls of the quartz tube. All reagents were used as commercially supplied.

Characterization of the carbonaceous materials was performed by transmission electron microscopy (TEM), thermal gravimetric analysis (TGA), Raman spectroscopy and X-ray photoelectron spectroscopy (XPS). BET was employed to establish the surface areas and pore volumes of the CNTs. TEM analysis were performed on a JEOL JEM-100S Electron Transmission Microscope at 80 kV and at varying magnifications. The TEM samples were dispersed in methanol using a sonicator and loaded onto a copper grid. The composition of the SCNMs formed was determined by counting at least 100 'shaped objects' per sample. These were randomly chosen from different TEM images. The methodology thus provides a crude but easy method of comparing the effect of reaction variables on the product distribution. Raman spectroscopy data was obtained from a Jobin-Yvon T6400 spectrometer. The excitation source was 636.4 nm from a tunable spectra Physics dye laser, while the backscattered light was dispersed using a 600 line/nm grating. TGA data were collected from a Perkin Elmer TGA analyzer in air at a heating rate of 10 °C/min. XPS analysis was carried out on a Physical Electronics Quantum 2000 analyser (CSIR, Pretoria) with resolution of 0.1 at.%.

3. Results and discussion

3.1. Crystal structure of 4-ferrocenylaniline

A single crystal of 4-ferrocenylaniline was grown by slow evaporation of a dichloromethane/hexane solution containing the compound. The crystal data was collected at 173 K and the least squares refinement of the structure gave a final *R* factor of 0.0221. The PLATON diagram of the molecule giving its numbering scheme is shown in Fig. 1. The summary of structural refinement data is provided as Supplementary material and the detailed crystal data (*cif* file) has been deposited with the Cambridge Data File # CCDC 680815.

4-Ferrocenylaniline was observed to crystallize in the orthorhombic crystal system showing four molecules per unit cell. The distance of the Fe atom from the centroids of the substituted (1.651 Å) and the unsubstituted cyclopentadienyl (Cp) (1.654 Å) ring for this compound were found to be generally longer than those for similar arylferrocene compounds such as 4-nitrophenylferrocene [28,29]. This could be due to the NH_2 group being an electron donating group, hence 'pumping' electrons to the metal center. This leaves the Fe center more negative causing repulsion of both the Cp rings leading to a lengthening of the Fe-centroid distances in an attempt to overcome the increasing electron cloud density induced by the NH_2 group. On the contrary, NO_2 on 4-nitrophenylferrocene is an electron withdrawing group, and therefore has an opposite impact on the bond lengths. The short C6–C11 (1.478(2) Å) length on 4-ferrocenyaniline does suggest a partial double bond character. This suggests the enhanced conjugation between the NH_2 on the phenyl and the Cp ring. This is also supported by the torsion angles which indicate that the Cp ring and the phenyl ring are fairly co-planar allowing for good overlap of π-electrons for bonding. The ferrocenyl moiety of the 4-ferrocenyaniline was found to be in a staggered conformation which is

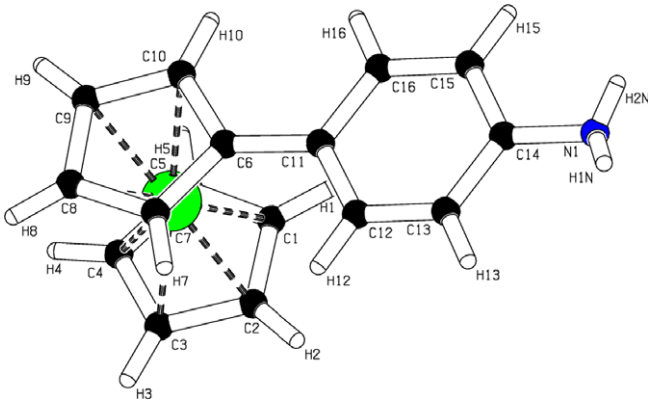

Fig. 1. Crystal structure for 4-ferrocenylaniline.

also not unusual. The packing diagram of 4-ferrocenyaniline shows discrete molecules packed in an ordered fashion and the only interactions obtained are those *via* normal Van der Waals contacts.

3.2. Synthesis and characterization of N-CNTs

N-doped carbon nanotubes were synthesized from solutions of 4-ferrocenylaniline in toluene (2.5 or 5.0 wt.% $FcPhNH_2$) or solutions of varying concentrations of aniline (0, 2.5, 5, 10, 15 or 25 wt.%) in toluene while keeping the concentration of ferrocene constant (2.5 wt.% FcH). Toluene, aniline and the cyclopentadienyl ligands provided the carbon for CNT growth. The catalysts used in this study are shown in Fig. 2.

3.2.1. TEM analysis

A reaction was recorded using FcH (2.5 wt.%) and toluene (no aniline) at 900 °C to provide base line data (Table 1). SEM images of the product obtained from both FcH and a FcH/aniline/toluene reaction are shown in Fig. 3. As can be seen, the product comprises mostly of CNTs. Further, whereas the FcH product shows good alignment of CNTs the sample made from the Fc/aniline mixture indicates alignment loss.

TEM analysis was used to examine the type, quality, size distribution and quantity (%) of the various SCNMs produced in the different synthesis reactions. In every instance MWCNTs were produced. TEM analysis allowed a facile measure of N doping to be determined. Nitrogen doping is known to significantly alter the morphological structure of CNTs, resulting in the formation of compartmentalized bamboo structures (Fig. 4). With FcH the SCNMs produced contain a modest yield of *non-compartmentalized* MWCNTs (Fig. 4a) together with nanofibers, nanospheres and amorphous carbon; with aniline, compartmentalized tubes are detected (Fig. 4b and c). At very low doping levels these bamboo structures may not be detected. The bamboo structures are produced by a base growth mechanism [30].

Replacement of FcH by either $FcPhNH_2$ or by $FcH/PhNH_2$ resulted in a substantial decrease in the total % of SCNMs formed, while the % CNTs formed increased. More importantly, N-CNTs were detected in both the above reactions and the degree of doping, determined by counting bamboo structured tubes is given in Table 1. The N-CNT diameters increased relative to the undoped CNTs. Fig. 4b and c provides low resolution TEM images of N-CNTs synthesized from the two different catalysts and reveals the bamboo compartments in both samples. Fig. 5 shows a high magnification TEM image of a N-CNT; the picture clearly reveals the tubular nature of the N-CNT as well as the compartment wall and the rough surface of the tube.

Doping reactions were performed with 5 wt.% catalyst solutions *in which the Fe content and Fe/N ratio were kept constant*. The TEM data for the SCNMs produced from FcH (3.33 wt.%)/$PhNH_2$ (1.67 wt.%) and from $FcPhNH_2$ (5 wt.%) have been compared, and the following differences have been noted:

(i) the total yield of SCNMs for $FcPhNH_2$ > $FcH/PhNH_2$;
(ii) the CNT yield for $FcH/PhNH_2$ < $FcPhNH_2$;
(iii) the CNT diameters for $FcPhNH_2$ > $FcH/PhNH_2$;
(iv) the % N doping for $FcPhNH_2$ > $FcH/PhNH_2$.

This indicates that the effect of the N hetero atom bound to the catalyst molecule can have a large impact on the size, type and distribution of SCNMs produced when compared to the case where the N hetero atom is not attached to the catalyst. The data obtained in the above reaction is consistent with the proximity of the N to the Fe playing a role in the formation of the N-CNTs. As will be described below, information from Raman spectroscopy is also consistent with this effect.

The data shown in Table 1 also allows for a comparison of the SCNMs produced at different concentrations viz. 2.5% and 5 wt.% $FcPhNH_2$ catalysts to be made (Table 1; and see below). Remarkable effects on tube formation and doping are to be noted.

The effect of systematically varying the aniline concentration on the MWCNT yield was investigated. Thus, TEM studies on the products formed from 1.25 to 25 wt.% concentrations of aniline in toluene revealed the following:

(i) The N-CNT diameters decreased (75–20 nm) as the % aniline increased from 1.25% to 25% i.e. larger concentrations of the N-source yielded CNTs with smaller diameters (Fig. 4). Similar effects were observed in a recent study when benzylamine was used as a nitrogen source [31].

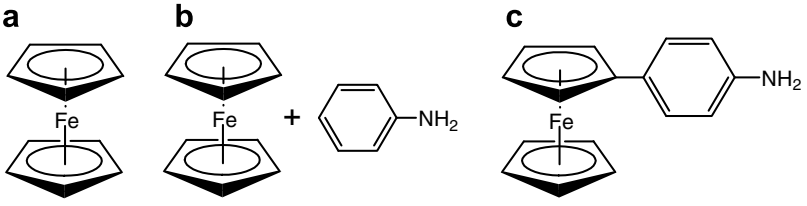

Fig. 2. The catalyst systems used with toluene as carbon source: (a) ferrocene (FcH); (b) ferrocene + aniline ($FcH/PhNH_2$) and (c) 4-ferrocenylaniline ($FcPhNH_2$).

Table 1
Summary of the yield and size distribution of SCNMs produced from different catalysts

Concentration (wt.%)	Fe/N molar ratio	SCNMs (%)	CNTs diameters (nm)	Yield (mg)	Degree of doping (%)
FcH (2.5)	1:1	30T, 20F, 45aC, 5S	60T, 80F, 300S	560	0
$FcPhNH_2$ (2.5)	1.1	45T, 30F, 25aC	65T, 95F, 210S	342	7
$FcPhNH_2$ (5)	1.1	72T, 18F, 10aC	55T, 80F	340	90
FcH (3.33) + $PhNH_2$ (1.67)	1:1	80T, 10F, 8aC, 2S	40T, 75F, 320S	240	1
FcH (2.5) + $PhNH_2$ (1.25)	1:1	35T, 30F, 30aC, 5S	75T, 100F	431	3
FcH (2.5) + $PhNH_2$ (2.5)	1:2	45T, 40F, 15aC	65T, 100F	397	5
FcH (2.5) + $PhNH_2$ (5)	1:4	50T, 40F, 10aC	60T, 95F	495	26
FcH (2.5) + $PhNH_2$ (10)	1:8	70T, 15F, 15aC	40T, 80F	521	95
FcH (2.5) + $PhNH_2$ (15)	1:12	80T, 15F, 5aC	25T, 70F	510	>99
FcH (2.5) + $PhNH_2$ (25)	1:20	70T, 20F, 10aC	20T, 70F	436	90

T: Nanotubes, F: Nanofibers, aC: Amorphous carbon and S: Nanospheres.

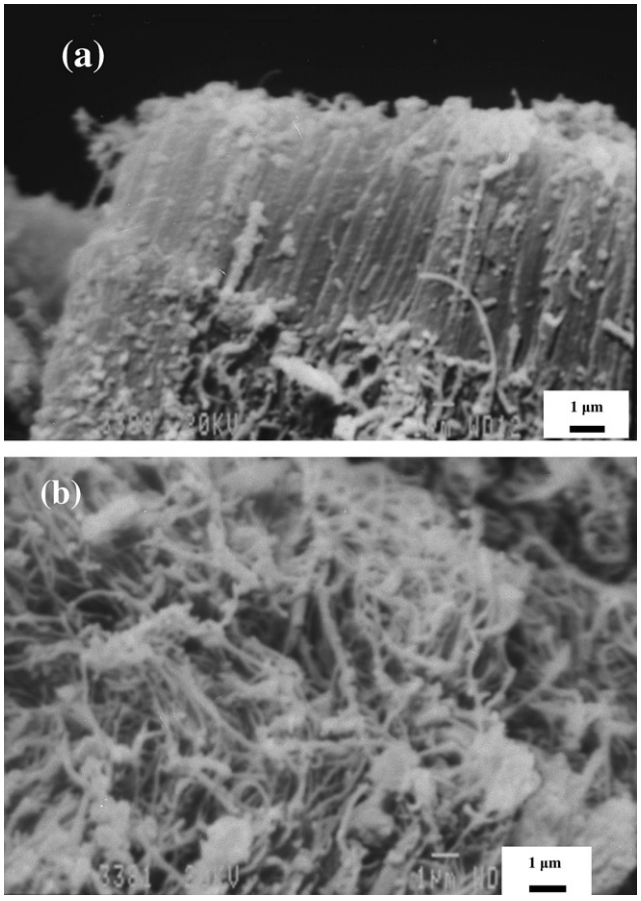

Fig. 3. SEM pictures of N-CNT bundles grown from; (a) FcH (2.5 wt.%) and FcH (2.5 wt.%)/$PhNH_2$ (15 wt.%).

(ii) The total yield varied in a non-linear manner with aniline concentration. An increase in aniline concentration favoured the production of more tubes. This is true until 25 wt.% aniline concentration was used; then a drop in N-CNT formation occurred.

(iii) The % doping increased with aniline concentration. It appears that a 15 wt.% aniline concentration is sufficient to produce close to 100% N-MWCNTs with a bamboo structure (Fig. 4b and c).

The distance between bamboo 'caps' was measured from TEM images (>100 measurements per sample) for the different samples and the average distances are reported in Table 2. It appears that the distance between the bamboo 'caps' within a tube is affected by the concentrations of the N source. An increase in % N source decreases the compartment distance. This is not unexpected and is consistent with the mechanism proposed for N-CNT growth [14]. It was also noted from the TEM analysis that some of the tubes contained metal nanoparticles (see Fig. 4c). The presence of the Fe nanoparticles is consistent with the synthesis of N-CNTs via a tip or base growth mechanism.

3.2.2. TGA studies

The thermal stabilities of the various products were evaluated by thermogravimetric analysis in air. Generally, decomposition of the SCNMs was observed from a temperature range of 500–610 °C. This accounts for most of the weight loss (*ca.* 90%). The thermal stability of the carbon nanostructures grown from FcH (2.5 wt.%)/$PhNH_2$ (1.5 wt.%) and $FcPhNH_2$ (2.5 wt.%) are compared in Fig. 6. The weight loss for the $FcPhNH_2$ sample at $T < 200$ °C is

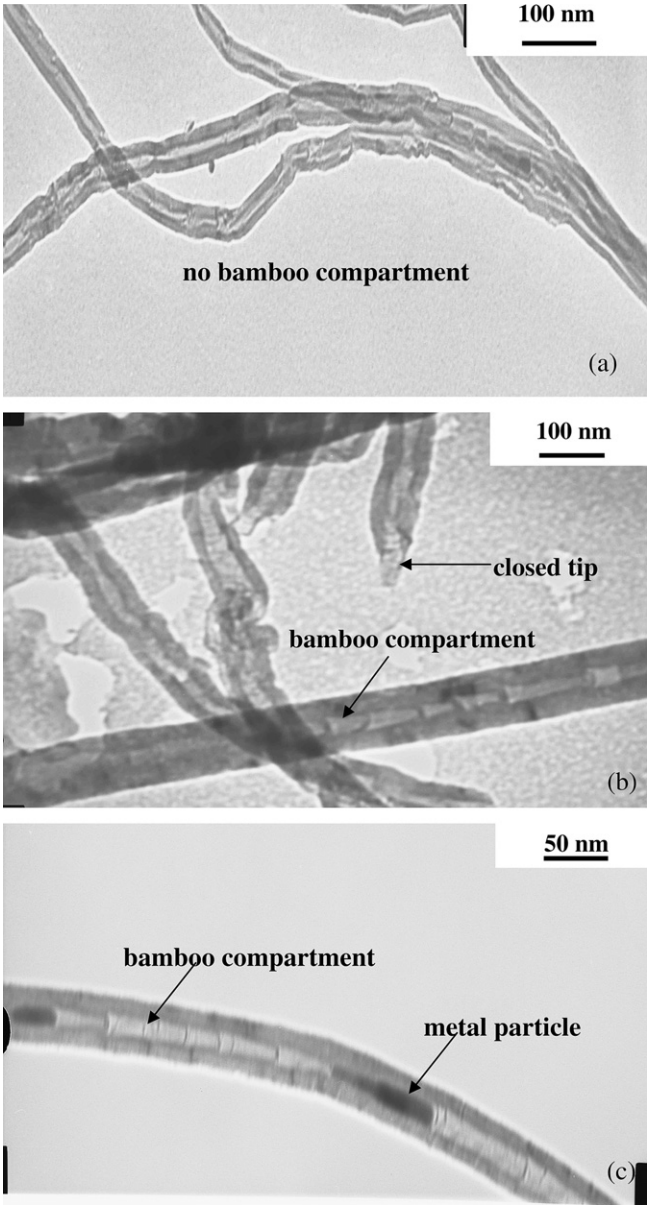

Fig. 4. TEM pictures of CNTs grown from (a) FcH (2.5 wt.%) (b) $FePhNH_2$ (2.5%) and (c) FcH (2.5 wt.%)/$PhNH_2$ (5 wt.%).

attributed to the loss of moisture from the material (Fig. 5). The SCNMs grown from $FcPhNH_2$ (2.5 wt.%) are less stable than those of FcH (2.5 wt.%)/$PhNH_2$ (1.25 wt.%) and this is attributed to the structural disorder introduced by the presence of N into the carbon lattice [32]. (The N-CNTs are also less thermally stable than the CNTs synthesized from FcH (not shown)). The residual weight (5–10%) observed in the TGA profiles is ascribed to FeO_x residues formed in air from the catalyst.

As expected, TGA profiles revealed that an *increase* in aniline concentration gave rise to the synthesis of less thermally stable N-CNTs (Figs. S3 and S4). For example, CNTs synthesized from 15 wt.% aniline started decomposing at 510 °C while those grown from 5 wt.% aniline started losing mass at 560 °C. This is due to the defect and disorder achieved by the introduction of reactive sites in the N-CNTs [33].

3.2.3. Raman spectroscopy

Raman spectroscopy is an excellent tool for investigating the graphitic nature of carbon materials. The Raman spectra generally

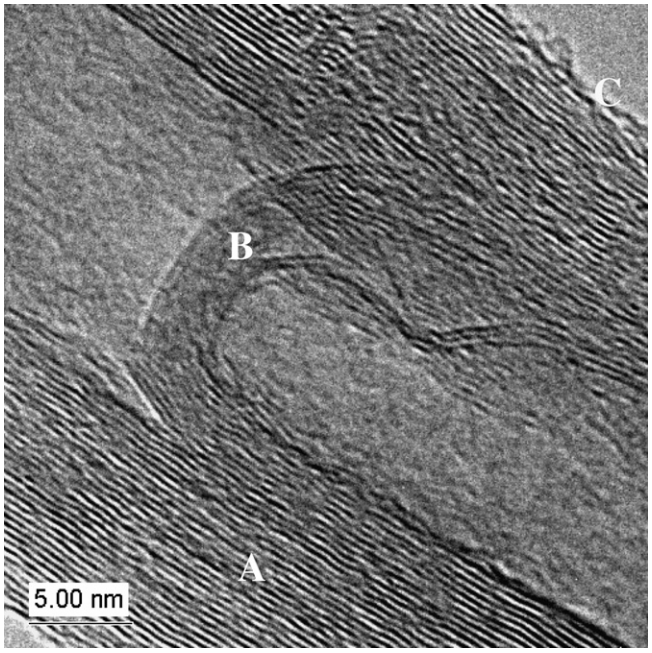

Fig. 5. High magnification TEM image of a N-CNT. The image clearly reveals the multi-walled nature of the tube A, the compartment wall B and the rough CNT surface C.

Table 2
Distance between N-CNT bamboo compartments

Concentration (wt.%)	Avg. distance between individual bamboo compartments (nm)
FcH (2.5)	None
$FcPhNH_2$ (2.5)	40
$FcPhNH_2$ (5)	31
FcH (3.33) + $PhNH_2$ (1.67)	45
FcH (2.5) + $PhNH_2$ (1.25)	62
FcH (2.5) + $PhNH_2$ (2.5)	34
FcH (2.5) + $PhNH_2$ (5)	32
FcH (2.5) + $PhNH_2$ (10)	43
FcH (2.5) + $PhNH_2$ (15)	18
FcH (2.5) + $PhNH_2$ (25)	20

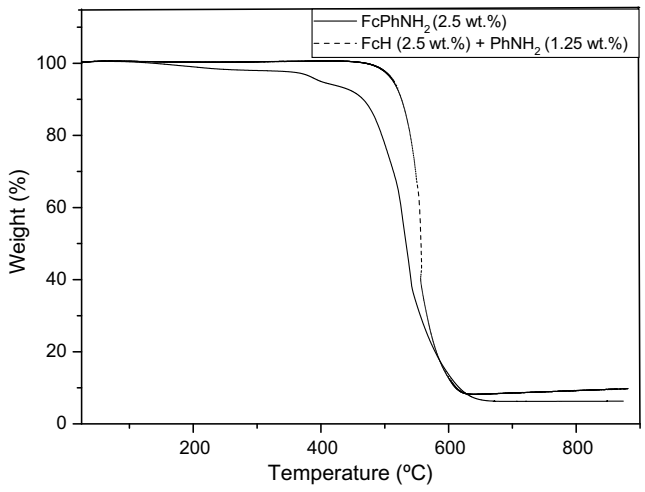

Fig. 6. TGA curves of CNTs grown from FcH (2.5 wt.%)/$PhNH_2$ (1.25 wt.%) and $FcPhNH_2$ (2.5 wt.%).

show two major peaks: a G-band at approximately 1590 cm^{-1} originating from the Raman active E_{2g} mode and a D-band at about 1350 cm^{-1} which is normally explained as a disorder-induced feature due to a finite particle size effect [33]. The I_D/I_G ratio represents the extent of disorder in the graphitic carbon. Thus, as the ratio approaches 0 the carbon will have a more ordered structure. Doping leads to disorder. Table 3 shows the positioning of the G- and the D-bands, their intensities as well as the I_D/I_G ratio of the carbon grown from the different catalyst combinations.

As shown in Table 3, when N-CNTs are produced from solutions with equivalent Fe/N ratios $FcPhNH_2$ gave a higher I_D/I_G ratio of (0.97) as compared to that of the mixture FcH (2.5 wt.%) + $PhNH_2$ (1.25 wt.%) (0.67) which in turn was higher than that of the undoped CNTs (0.63) (see also Fig. S2). This implies that N-CNTs produced from $FcPhNH_2$ were more disordered than that produced from FcH/$PhNH_2$. In the case of the FcH/$PhNH_2$ mixtures, the I_D/I_G ratios (Table 2) suggest that, as the concentration of aniline increased, the degree of disorder also increased. Indeed, the products produced with 1.25 wt.%, 5 wt.% and 15 wt.%, aniline concentrations give rise to I_D/I_G ratios of 0.67, 0.87 and 1.06, respectively. Extrapolation of the graph of Raman ratios also suggests that $FcPhNH_2$ (2.5 wt.%) is similar to FcH + $PhNH_2$ when the $PhNH_2$ concentration is *ca.* = 7.5 wt.%. Thus the impact of having the aniline attached to or separate from the ferrocene leads to a comparative 2–5× increase in N doping.

3.2.4. XPS and CN analysis

XPS and CN elemental analyses were conducted on the as-synthesized SCNMs to investigate the N-content in the CNTs. These techniques demonstrate the presence of quantifiable amounts of N in the tubes. N concentrations for the tubes were approximately 1.00 at.% (Table 4). For example, XPS analysis of FcH (2.5 wt.%)/$PhNH_2$ (>15 wt.%) gave >1% N content. The CN analysis similarly gave N atomic concentrations (%) of 1.07 and 1.05 for the $PhNH_2$ (15 wt.%) and $PhNH_2$ (25 wt.%) samples respectively. The C/N ratio of the N-CNTs produced by these two catalysts, were calculated to be 84 and 88. However, at lower concentrations of aniline (<2.5 wt.%) no nitrogen was detected in any of the samples by the two techniques, indicating much larger C/N ratios.

XPS analysis has the potential to give information about the hybridisation state of the N in the N-CNTs. According to Jang et al. [34], the type of N observed at high N concentrations in CNTs has been shown to be sp^3 hybridized; at lower N concentrations, a sp^2 signal for N was observed. The above results were obtained using NH_3/C_2H_2 reactant mixtures over a Fe/SiO_2 catalyst [34]. In this study the XPS data revealed that use of the 15% aniline solution gave an XPS signal for nitrogen consistent only with sp^2 hybridized N while a 25% aniline solution gave two nitrogen XPS signals (50/50) consistent with both sp^2 and sp^3 nitrogen. This suggests that chemical reactions that can be used to functionalize N-CNTs will give different reactions for the N-CNTs produced with different N contents.

Table 3
D- and G-band positions and I_D/I_G ratios of CNTs grown at different catalyst concentrations

Catalyst conc. (wt.%)	D-band (cm^{-1})	G-band (cm^{-1})	I_D/I_G Ratio
FcH (2.5)	1356	1587	0.63
$FcPhNH_2$ (2.5)	1364	1587	0.97
$FcPhNH_2$ (5)	1351	1592	1.02
FcH (3.33) + $PhNH_2$ (1.67)	1358	1587	0.72
FcH (2.5) + $PhNH_2$ (1.25)	1358	1589	0.67
FcH (2.5) + $PhNH_2$ (2.5)	1358	1587	0.86
FcH (2.5) + $PhNH_2$ (5)	1359	1591	0.87
FcH (2.5) + $PhNH_2$ (10)	1360	1597	1.05
FcH (2.5) + $PhNH_2$ (15)	1357	1596	1.06
FcH (2.5) + $PhNH_2$ (25)	1353	1596	0.99

Table 4
Nitrogen content for the N-CNTs synthesized from the various catalysts

Precatalyst (wt.%)	XPS (N at.%)	CN (N at.%)
$FcPhNH_2$ (2.5)	ND	ND
FcH (2.5) + $PhNH_2$ (1.25)	ND	ND
FcH (2.5) + $PhNH_2$ (15)	1.50	1.07
FcH (2.5) + $PhNH_2$ (25)	1.00	1.05

ND: not detected.

Table 5
Surface areas and pore volumes of N-CNTs grown at different catalyst concentrations

Catalyst conc. (wt.%)	Surface area (m^2/g)	Pore volume (cm^3/g)
FcH (2.5)	18.9	0.047
$FcPhNH_2$ (2.5)	25.6	0.088
$FcPhNH_2$ (5)	14.2	0.063
FcH (3.33) + $PhNH_2$ (1.67)	32.4	0.231
FcH (2.5) + $PhNH_2$ (1.25)	19.2	0.062
FcH (2.5) + $PhNH_2$ (2.5)	19.9	0.091
FcH (2.5) + $PhNH_2$ (5)	24.0	0.102
FcH (2.5) + $PhNH_2$ (10)	26.5	0.085
FcH (2.5) + $PhNH_2$ (15)	29.9	0.182
FcH (2.5) + $PhNH_2$ (25)	30.2	0.182

3.2.5. BET surface area and pore volume

The surface area and pore volume data for the as-synthesized N-CNTs were obtained using the Brunauer Emmett Teller (BET) method (Table 5). As expected the surface area and the pore volumes of the N-CNTs increased significantly as the aniline concentration increased. For example, the surface area for FcH (2.5 wt.%)/$PhNH_2$ (5 wt.%) = 24.0 m^2/g while that for 25 wt.% = 30.2 m^2/g. This is related to (i) the observed decrease in diameter of the N-CNTs and (ii) the more disordered CNT surface as the aniline concentration increased (Table 1). The surface area of the sample produced from $FcPhNH_2$ (2.5 wt.%) is similar to that of the sample produced from *ca.* = FcH (2.5 wt.%)/$PhNH_2$ (10 wt.%). This result is in agreement with the correlations observed from the Raman data presented in Table 3.

4. Conclusions

We have studied the effect of varying the N-source concentration on the production of N-doped CNTs and other SCNMs in a CVD reactor. Successful N-doping was evidenced by the presence of compartmentalized bamboo structures in the CNT walls. A ferrocene/aniline catalyst (15 wt.%) produced predominantly pure N-CNTs with only small amounts of amorphous carbon and other SCNMs. Generally, the Raman spectra of the as-synthesised N-CNTs showed a low degree of graphitization indicating the presence of defects and disorder in the CNT walls. XPS analysis demonstrated the presence of quantifiable amounts of N in the tubes. The study thus reveals that the diameters of the tubes can be controlled by systematically varying the N source concentration. More significantly a higher N content is achieved by using the aniline substituted ferrocene as a catalyst when compared to ferrocene/aniline mixtures. A *ca.* 2–5× increase was determined in N content using similar catalyst concentrations.

Acknowledgements

The authors wish to thank the DST/NRF Centre of Excellence in Strong Materials and the University of the Witwatersrand for financial support. They also wish to extend their gratitude to Dr Manuel Fernandes for the technical assistance in acquiring and refining the 4-ferrocenylaniline crystal data and structure. Werner Jordaan, Surface Analysis Group at the CSIR (Pretoria) is gratefully acknowledged for performing the XPS analysis. Thanks also go to Prof. Mike Witcomb, Electron Microscope Unit, University of the Witwatersrand for recording the high magnification TEM image.

Appendix A. Supplementary material

CCDC 680815 contains the supplementary crystallographic data for 4-ferrocenylaniline. These data can be obtained free of charge from The Cambridge Crystallographic Data Centre via www.ccdc.cam.ac.uk/data_request/cif. Supplementary data associated with this article can be found, in the online version, at doi:10.1016/j.jorganchem.2008.06.015.

References

[1] (a) S. Iijima, T. Ichihashi, Nature 363 (1993) 603;
(b) D.S. Bethune, C.H. Kiang, M.S. De Vries, G. Gorman, R. Savoy, J. Vazquez, R. Beyers, Nature 363 (1993) 605;
(c) H.P. Boehm, Carbon 35 (1997) 581.
[2] (a) R. Saito, G. Dresselhaus, M.S. Dresselhaus, Physical Properties of Carbon Nanotubes, Imperial College Press., London, 1998;
(b) G. Cao, Nanostructures and Nanomaterials: Synthesis, Properties & Applications Imperial College Press, London, 2004;
(c) M.S. Dresselhaus, G. Dresselhaus, P.C. Eklund, Science of Fullerenes and Carbon Nanotubes, Academic Press, San Diego, 1996;
(d) M.J. O'Connell, Carbon Nanotubes: Properties and Applications, Taylor & Francis Group, LLC, 2006.
[3] (a) A.M. Thayer, Chem. Eng. News (2007) 29. November;
(b) J. Evans, Chem. World (2007) 17. November.
[4] (a) P. Nikolaev, J. Bronikowski, R.K. Bradley, F. Rohmund, D.T. Colbert, K.A. Smith, R.E. Smalley, Chem. Phys. Lett. 313 (1999) 91;
(b) O.A. Nerushev, M. Sveningsson, L.K.L. Falk, F. Rohmund, J. Mater. Chem. 11 (2001) 1122.
[5] (a) S. Amelinckx, X.B. Zhang, D. Bernaerts, X.F. Zhang, V. Ivanov, J.B. Nagy, Science 265 (1994) 635;
(b) A.C. Dupuis, Prog. Mater. Sci. 50 (2005) 929;
(c) J.B. Park, G.S. Choi, Y.S. Cho, S.Y. Hong, D. Kim, S.Y. Choi, J.H. Lee, K.I. Cho, J. Cryst. Growth 244 (2002) 211;
(d) H. Dai, Surf. Sci. 500 (2002) 218;
(e) A.M. Cassell, J.A. Raymakers, J. Kong, H. Dai, J. Phys. Chem. B 103 (1999) 6484;
(f) Q.W. Li, H. Yan, Y. Cheng, J. Zhang, Z.F. Liu, J. Mater. Chem. 12 (2002) 1179;
(g) J.F. Colomer, C. Stephan, S. Lefrant, G. Van, I. Willems, Z. Konya, C. Laurent, J.B. Nagy, Chem. Phys. Lett. 317 (2000) 83.
[6] (a) K.C. Mondal, N.J. Coville, Encyclopedia of Nanoscience and Nanotechnology, American Scientific Publishers, California, USA, in press.;
(b) A. Govindaraj, C.N.R. Rao, Pure Appl. Chem. 74 (2002) 1571;
(c) V.O. Nyamori, S.D. Mhlanga, N.J. Coville, J Organometal. Chem. 693 (2008) 2205.
[7] (a) T.M. Keller, S.B. Qadri, Chem. Mater. 16 (2004) 1091;
(b) M.S. Mohlala, X.Y. Liu, M.J. Witcomb, N.J. Coville, Appl. Organomet. Chem. 21 (2007) 275;
(c) X.Y. Liu, B. C Huang, N.J. Coville, Fullerenes Nanotubes Carbon Nanostruct. 10 (2002) 339.
[8] M. Laskoski, T.M. Keller, S.B. Qadri, Carbon 45 (2007) 443.
[9] (a) M.S. Mohlala, X.Y. Liu, J.M. Robinson, N.J. Coville, Organometallics 24 (2005) 972;
(b) V.O. Nyamori, N.J. Coville, Organometallics 26 (2007) 4083.
[10] M.S. Mohlala, X.Y. Liu, N.J. Coville, J. Organomet. Chem. 691 (2006) 4768.
[11] M. Reyes-Reyes, N. Grobert, R. Kamalakaran, T. Seeger, D. Golberg, M. Rühle, Y. Bando, H. Terrones, M. Terrones, Chem. Phys. Lett. 21 (2004) 67.
[12] O. Stephen, P.M. Ajavan, C. Colliex, Ph. Redlich, J.M. Lambert, P. Bernier, P. Letin, Science 266 (1994) 1683.
[13] R.B. Sharma, D.J. Late, D.S. Joag, A. Govindaraj, C.N.R. Rao, Chem. Phys. Lett. 428 (2006) 102.
[14] C.P. Ewels, M. Glerup, J. Nanosci. Technol. 5 (2005) 1345.
[15] Q.-H. Yang, P.-X. Liu, M. Unno, S. Yamauchi, R. Saito, T. Kyotani, Nano Lett. 5 (2005) 275.
[16] R.V. Parthasarathy, K.L.N. Phani, C.R. Martin, Adv. Mater. 7 (1995) 896.
[17] S. Point, T. Minea, B. Bouchet-Fabre, A. Granier, G. Turban, Diamond Relat. Mater. 14 (2005) 891.
[18] F. Villalpando-Paez, A. Zamudio, A.L. Elias, H. Son, E.B. Barros, S.G. Chou, Y.A. Kim, H. Muramatsu, T. Hayashi, J. Kong, H. Terrones, G. Dresselhaus, D. Endo, M. Terrones, M.S. Dresselhaus, Chem. Phys. Lett. 424 (2006) 345.
[19] (a) C.N.R. Rao, A. Govindaraj, G. Gundiah, S.R.C. Vivekchand, Chem. Eng. Sci. 59 (2004) 4665;
(b) F.L. Deepak, A. Govindaraj, C.N.R. Rao, Chem. Phys. Lett. 345 (2001) 5;
(c) C.N.R. Rao, A. Govindaraj, Acc. Chem. Res. 35 (2002) 998.
[20] T. Lanez, P.L. Pauson, J. Chem. Soc., Perkin Trans. I (1990) 2437.
[21] A.N. Nesmeyanov, E.G. Perevalova, R.V. Golovnya, L. Shilovtseva, Dokl. Akad. Nauk SSSR 102 (1955) 535.

[22] Bruker, APEX2, Version 2.0-1, Bruker AXS Inc., Madison, WI, USA, 2005.
[23] Bruker, SAINT-NT, Version 6.0 (includes XPREP and SADABS), Bruker AXS Inc., Madison, WI, USA, 2005.
[24] Bruker, SHELXTL, Version 5.1 (includes XS, XL, XP, XSHELL), Bruker AXS Inc., Madison, WI, USA, 1999.
[25] A.L. Spek, J. Appl. Crystallogr. 36 (2003) 7.
[26] L.J. Farrugia, J. Appl. Crystallogr. 30 (1997) 565.
[27] M.S. Mohlala, N.J. Coville, J. Organomet. Chem. 692 (2007) 2965.
[28] J.F. Gallagher, G. Ferguson, S.Z. Ahmed, C. Glidewell, A. Lewis, Acta Crystallogr., Sect. C 53 (1997) 1772.
[29] R.M.G. Roberts, J. Silver, B.M. Yamin, M.G.B. Drew, U. Eberhardt, J. Chem. Soc., Dalton Trans. (1988) 1549.
[30] P.J. Harris, Carbon 45 (2007) 229.
[31] X.Y. Tao, X.B. Zhang, F.Y. Sun, J.P. Cheng, F. Liu, Z.Q. Luo, Diamond Relat. Mater. 16 (2007) 425.
[32] (a) R. Kurt, A. Karini, Chem. Phys. Chem. 2 (2001) 388;
(b) X. Ma, E.G. Wang, Appl. Phys. Lett. 78 (2001) 978.
[33] (a) S. Maldonado, S. Morin, K.J. Stevenson, Carbon 44 (2006) 1429;
(b) S. Choi, K.H. Park, S. Lee, K.H. Koh, J. Appl. Phys. 92 (2002) 4007.
[34] J.W. Jang, C.E. Lee, S.C. Lyu, T.J. Lee, C.J. Lee, Appl. Phys. Lett. 84 (2004) 2877.